

To see the latest GeoStudio learning content, visit <u>Seequent Learning Centre</u> and search the catalogue for "GeoStudio".

Introduction

Stresses and displacements are determined numerically for the case of a cylindrical hole in an infinite Mohr-Coulomb material subjected to an isotropic in situ stress field. The analytical solution for this problem is provided by Salençon (1969) for associated and nonassociated plastic flow. The problem tests the Mohr-Coulomb model with applied field stresses in plane-strain conditions imposed in Sigma/W.

The material is assigned the following properties:

Young's modulus (E) 7 GPa Poisson's ratio (v) 0.25 Effective cohesion (c) 2.5 kPa Effective friction angle (ϕ) 30° Dilation angle (ψ) 0° and 30°

The analytical solution for stresses and displacements are given below.



Yield zone radius	$R_0 = a \left[\frac{2}{K_p + 1} \frac{1 + \frac{q}{P_0} k_p}{\frac{P_i}{P_0} + \frac{q}{P_0} k_p} \right]_{k_p}$
Hole radius	$\begin{bmatrix} P_0 & P_0 \end{bmatrix}$
Absolute value of in situ isotropic stress	P_0
Pressure inside the hole	P_i
	$K_p = \frac{1 + \sin\phi}{1 - \sin\phi}$
	$k_p = \frac{1}{K_p - 1}$
	$q = 2 c \sqrt{K_p}$
Distance from the hole centre	r
Radial stress at elastic/plastic interface	$\sigma_{re} = -\frac{1}{K_p + 1} (2 P_0 - q)$
Radial stress in the plastic zone	$\sigma_r = P_0 \left[\frac{q}{P_0} k_p - \left(\frac{P_i}{P_0} + \frac{q}{P_0} k_p \right) \left(\frac{r}{a} \right)^{K_p - 1} \right]$
Tangential stress in the plastic zone	$\sigma_{\theta} = P_0 \left[\frac{q}{P_0} k_p - K_p \left(\frac{P_i}{P_0} + \frac{q}{P_0} k_p \right) \left(\frac{r}{a} \right)^{K_p - 1} \right]$
Radial stress in the elastic zone	$\sigma_r = -P_0 + (P_0 - \sigma_{re}) \left(\frac{R_0}{r}\right)^2$
Tangential stress in the elastic zone	$\sigma_{\theta} = -P_0 \left[\frac{\sigma_r}{P_0} + 2 \right]$
Radial displacement in the plastic zone	$u_r = -\frac{P_0}{2G} r \chi \left(\frac{r}{a}\right)$
Shear modulus	$G = \frac{E}{2(1+\nu)}$
	$\chi\left(\frac{r}{a}\right) = (2\nu - 1)\left(1 + \frac{q}{P_0}k_p\right)$
	$+\frac{(1-\nu)(K_p^2-1)}{(K_p+K_{ps})} \left(\frac{P_i}{P_0} + \frac{q}{P_0} k_p\right) \left(\frac{R_0}{a}\right)^{K_p+K_{ps}} \left(\frac{r}{R_0}\right)^{-K_{ps}-1}$
	$+ \left[(1 - \nu) \frac{K_p K_{ps} - 1}{K_p + K_{ps}} - \nu \right] \left(\frac{P_i}{P_0} + \frac{q}{P_0} k_p \right) \left(\frac{r}{a} \right)^{K_p - 1}$
	$K_{ps} = \frac{1 + \sin\psi}{1 - \sin\psi}$



Radial displacement in the elastic zone	$u_r = -\frac{P_0}{2G} \left(1 + \frac{\sigma_{re}}{P_0} \right) \frac{R_0^2}{r}$
	20\ 10)1

Numerical Simulation

For modelling purposes, the problem is defined by the domain sketched in Figure 1. The model is subjected to an isotropic in situ stress field of magnitude P_0 = 25 kPa and contains a hole of radius a = 1 m. The hole is not pressurized (P_i = 0 kPa). The model takes advantage of quarter symmetry. In the analytical solution, infinite boundaries are assumed but in the Sigma/W model the external boundaries are placed at 10 m from the hole centre.

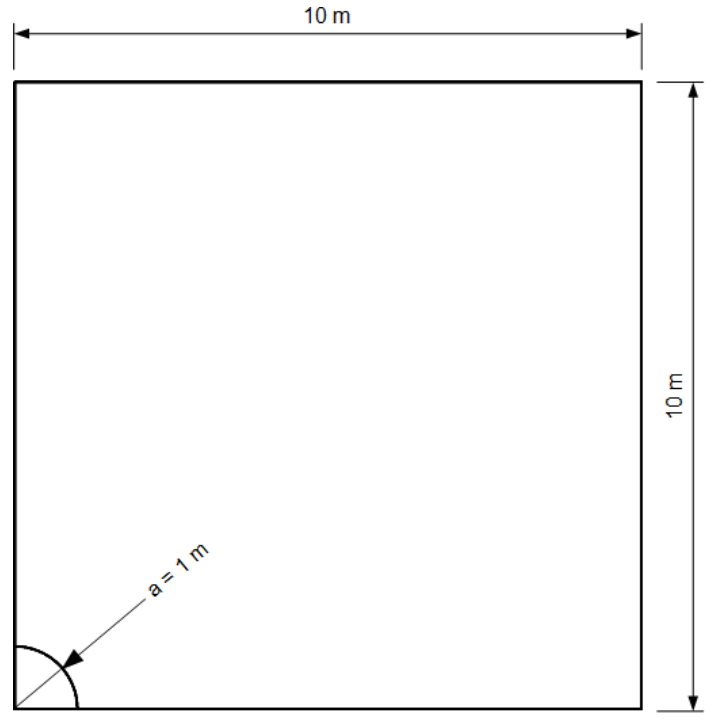


Figure 1. Model geometry.

The GeoStudio configuration for this model is shown in Figure 2. The 3D geometry tools were used to construct the geometry and a vertical section was cut through the 3D model for the 2D plane strain geometry.



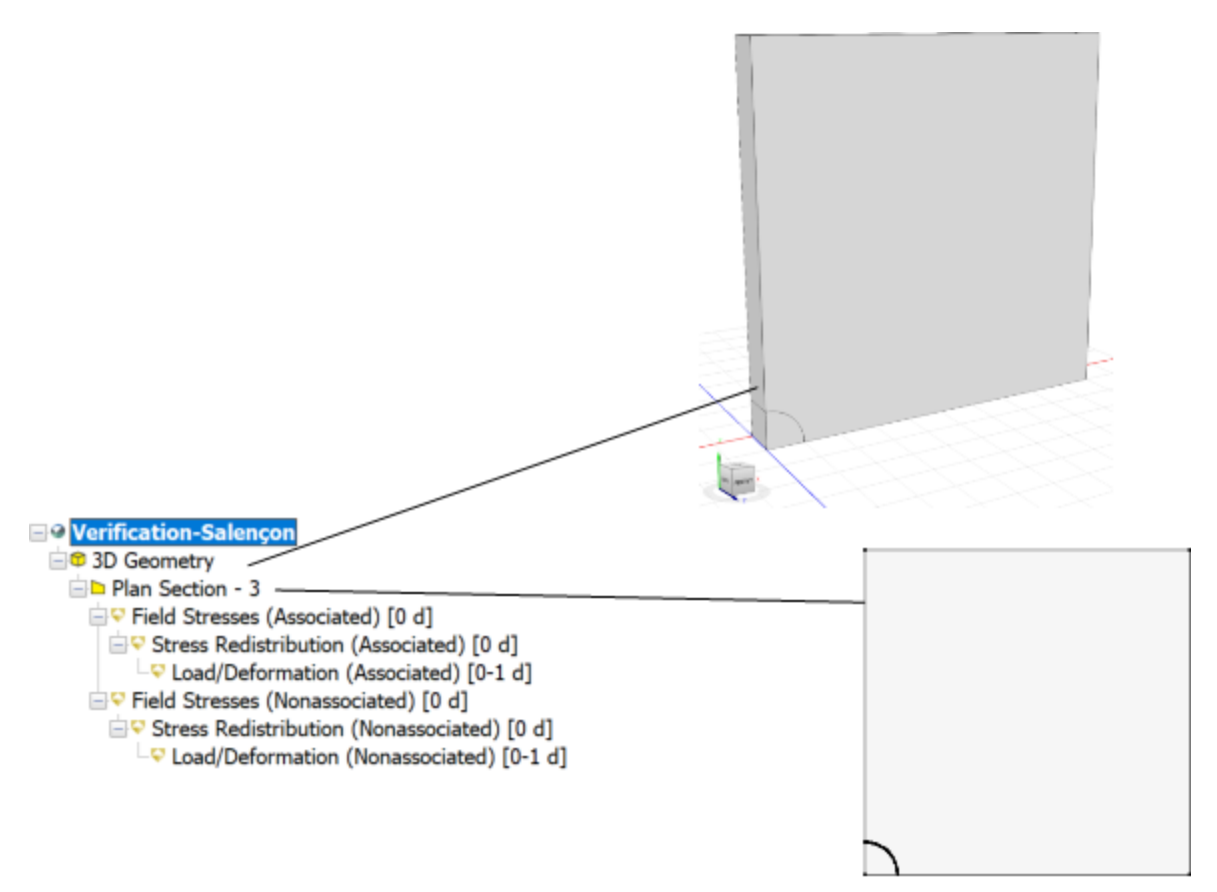


Figure 2. GeoStudio analysis tree, 3D geometry, and vertical cross section through the 3D geometry.

Figure 3 shows the In Situ analysis of the GeoStudio model. In the Define Project options, an In Situ analysis is selected with the Field Stresses method. The entire model, including the yet to be excavated circular opening, are assigned Mohr-Coulomb material. This analysis method allows a user defined constant stress field (see Define > Field Stresses in the GeoStudio menu) to be applied to the model. Field stresses are applied to the model through Draw > Field Stresses. Areas where field stresses have been applied are shown cross-hatched in red. X-extent model boundaries are fixed in the x-direction and y-extent model boundaries are fixed in the y-direction.

The Field Stress analysis does not account for gravitational effects and unit weight of defined materials is ignored. The model is in equilibrium with the applied and initial stresses and boundary conditions. As a result, solving this step does not require iterations. In more advanced analyses, especially when using a plastic material, such as this, the model may not be in equilibrium for a number of reasons, such as field stress magnitudes exceeding material strength or inappropriate boundary conditions. In cases where plastic material is used, such as this, it is advisable to run a Stress Redistribution analysis using the Stress Correction method immediately following the In Situ Field Stress Analysis. The Stress Correction analysis should be checked for yielding conditions (Figure 4). It is advisable to start from a well defined stress state with field stresses, where the model remains in the elastic state.



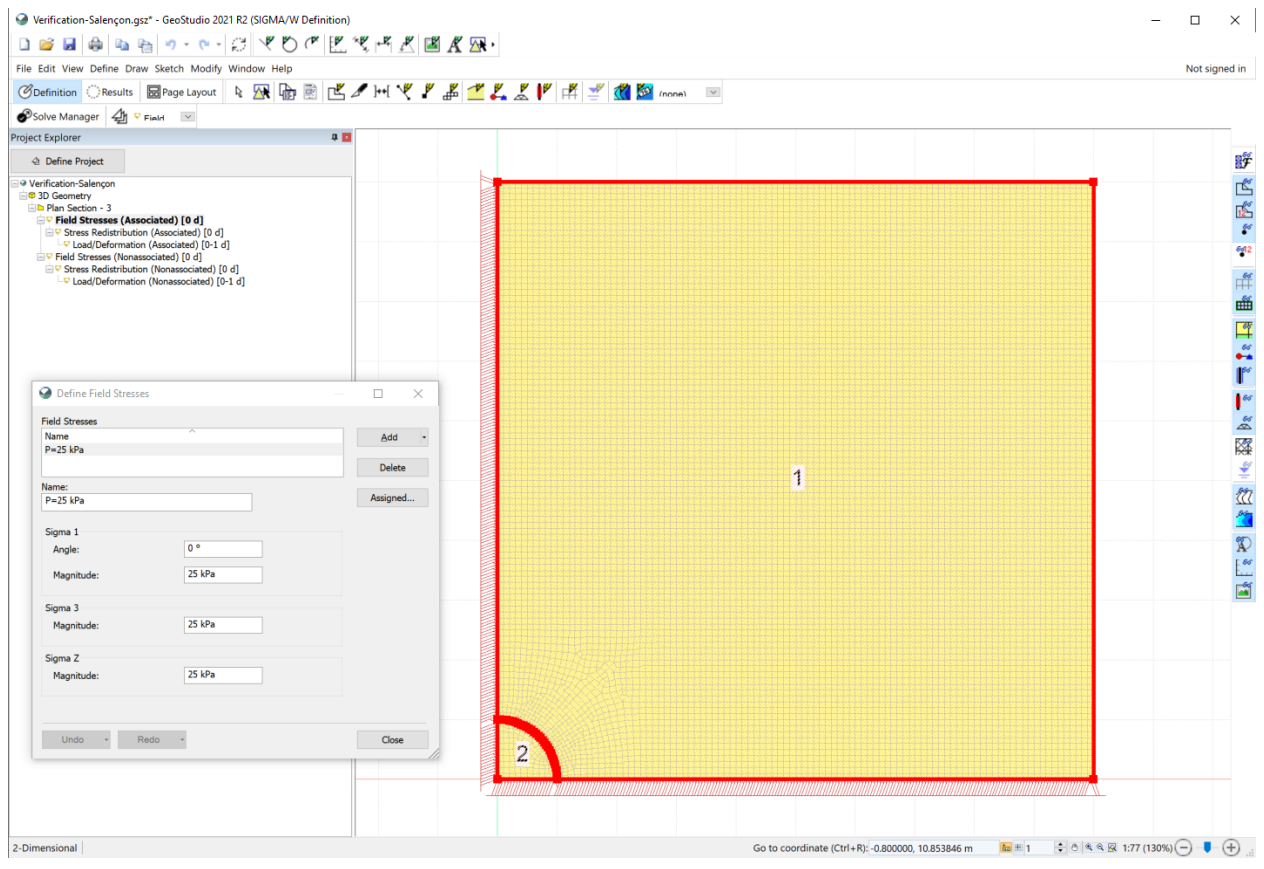


Figure 3. Field Stress definition, model mesh, and boundary conditions for In Situ analysis.



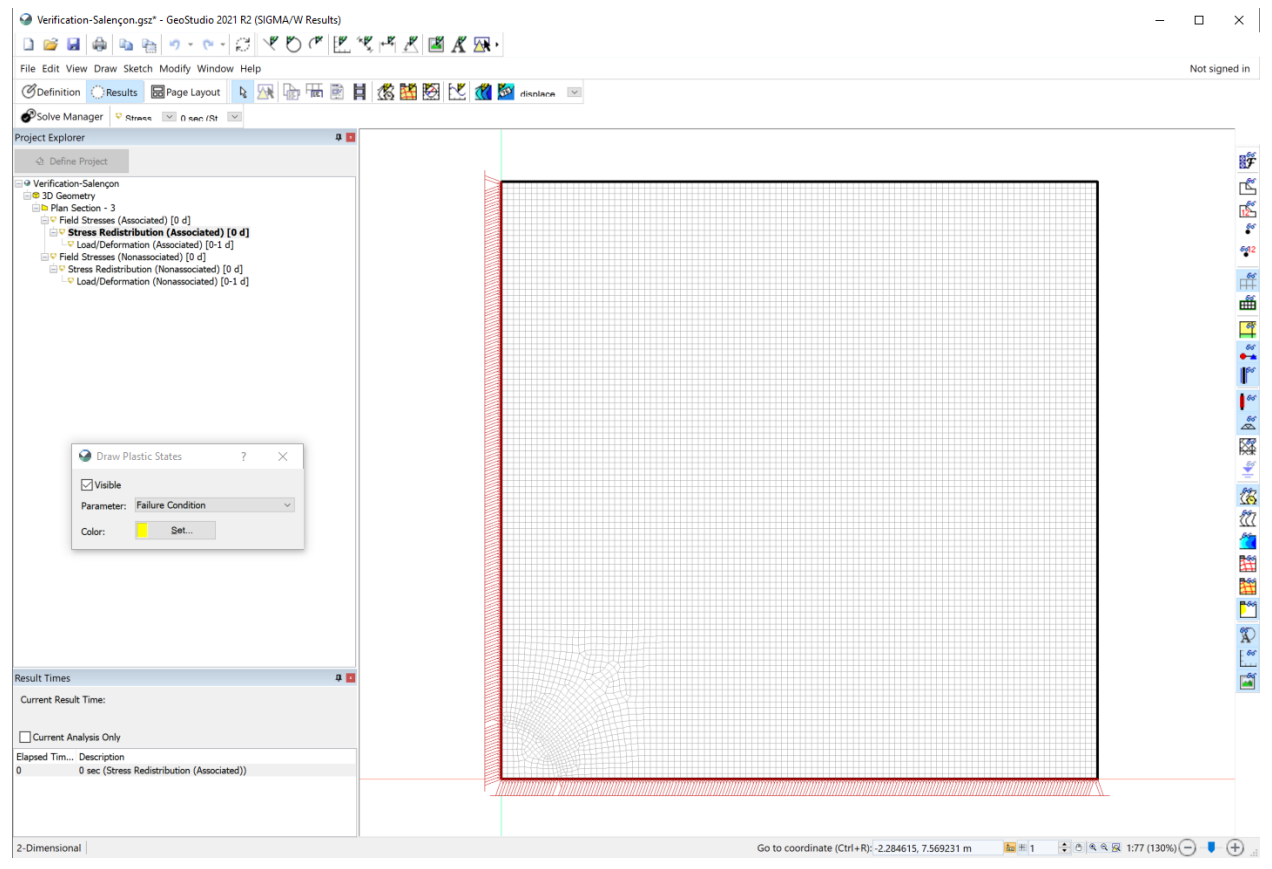


Figure 4. Stress Redistribution analysis and checking for yielded areas in the model.

A Load/Deformation analysis is run after the Stress Redistribution analysis, Figure 5 . The material in the circular opening is removed (the Mohr-Coulomb material is unassigned). The material deforms according to the load imbalance caused by the material removal.



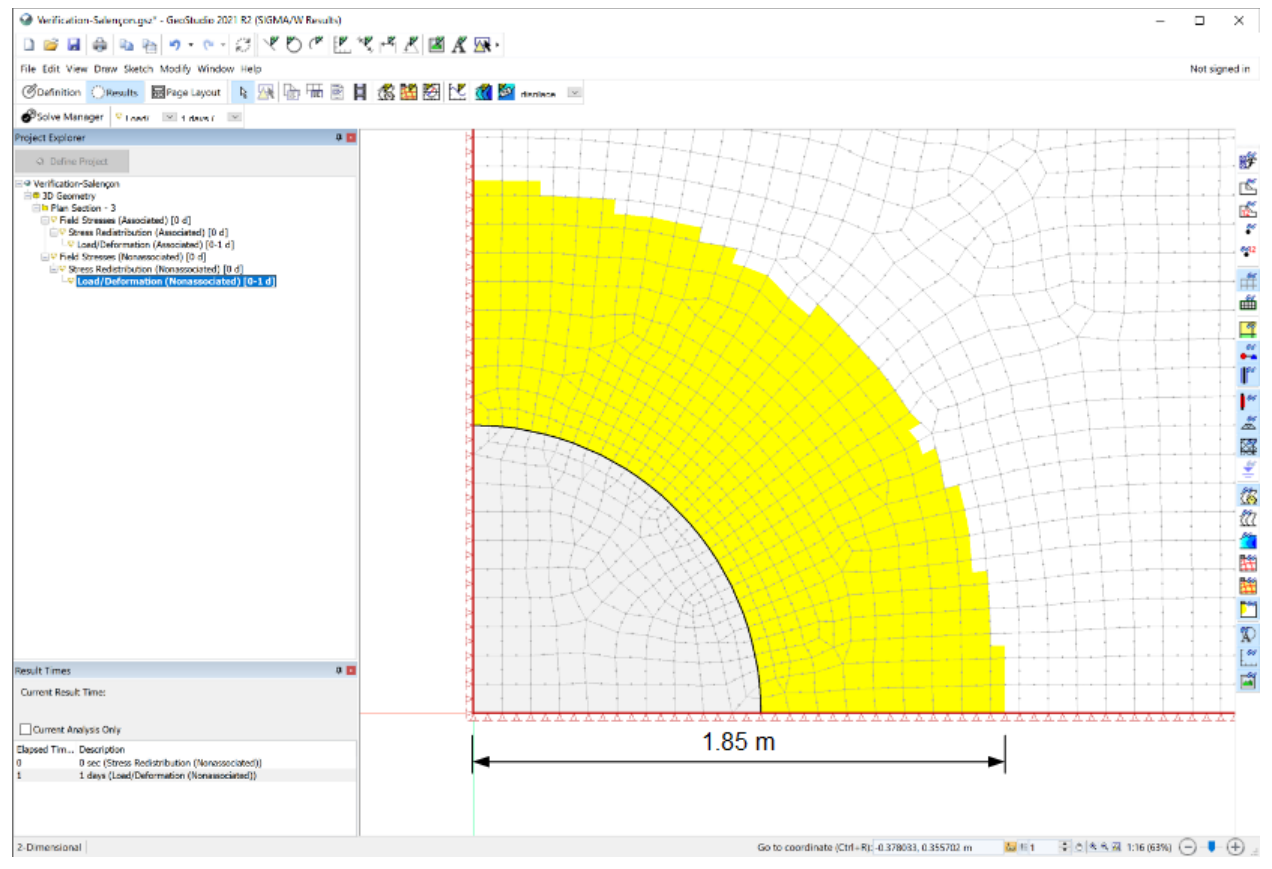


Figure 5. Load/Deformation analysis showing yielded area in yellow.

Results and Discussion

Displacements and stresses along a radial line were extracted from the GeoStudio model and processed by a Python script to compare with analytical results (Figure 6 - Figure 9). The analytical yield zone extent is 1.84 m (yellow area in Figure 5) for the associated and the nonassociated flow cases.

In the graphs below, stresses are normalized to the isotropic field stress, $^{P}_{0}$. The match with analytical results, including the yield extent, is good, and the error can be made arbitrarily small by using a finer discretization and moving the model boundaries further out.



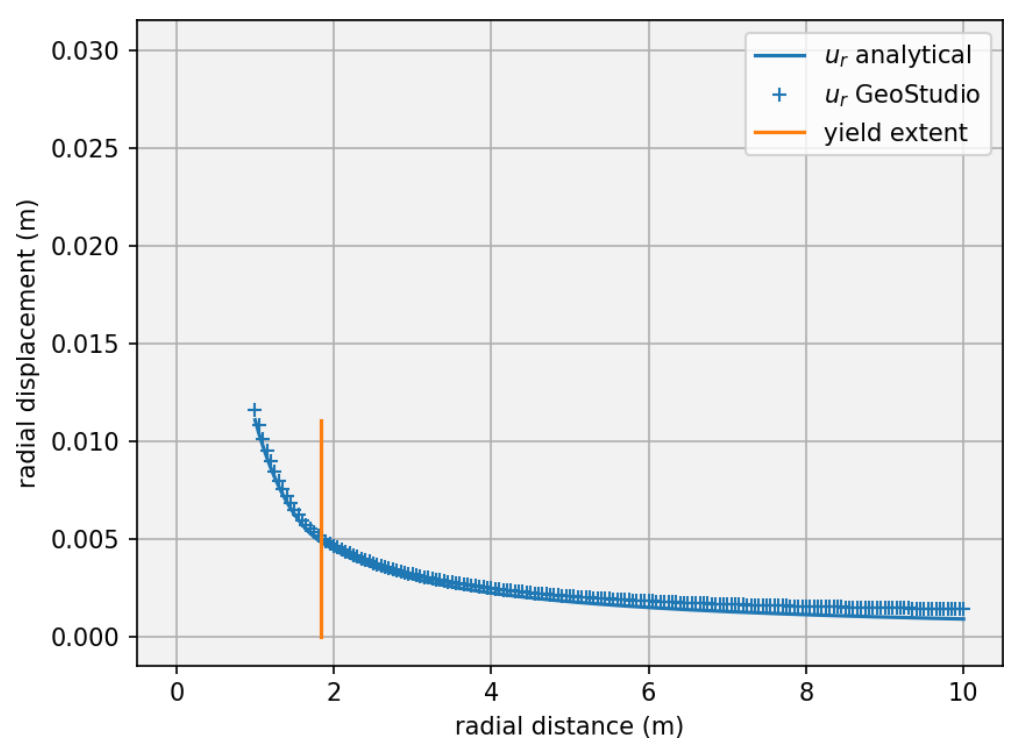


Figure 6. Radial displacement versus radial distance. Nonassociated flow, dilation = 0°.

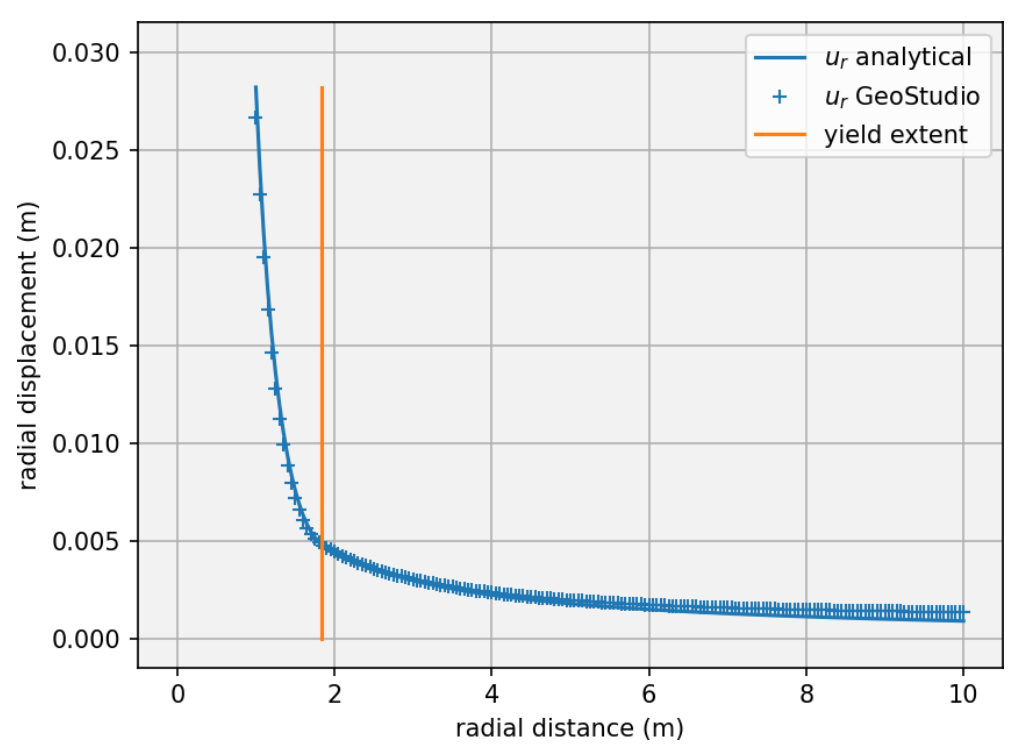


Figure 7. Radial displacement versus radial distance. Associated flow, dilation = 30°.



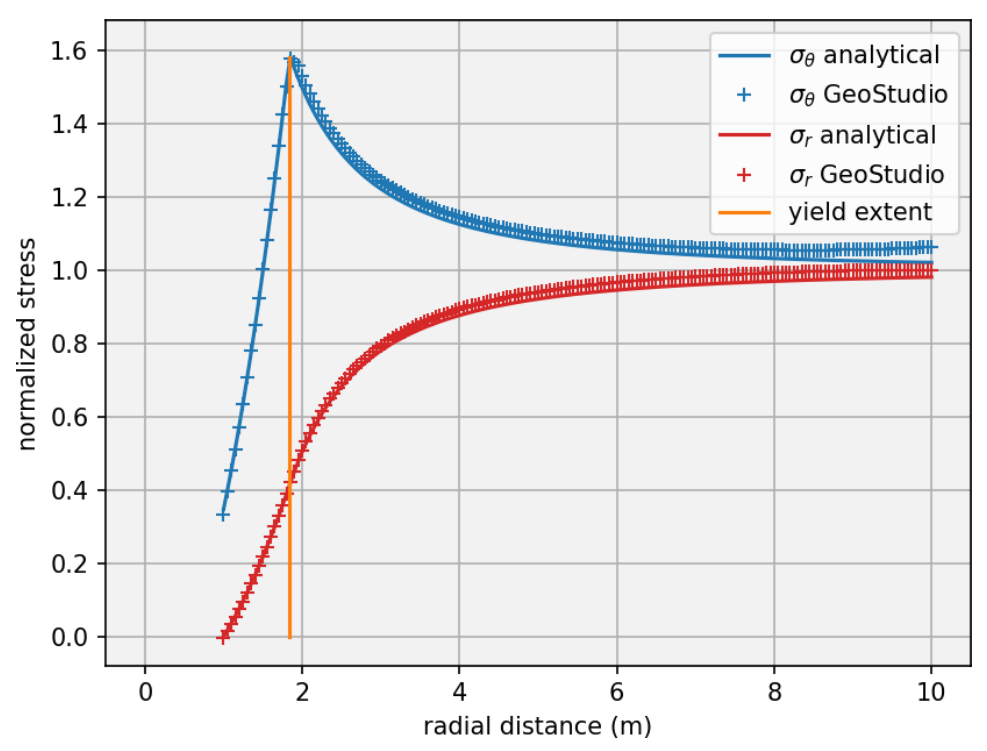


Figure 8. Normalized radial and tangential stress versus radial distance. Nonassociated flow, dilation = 0°.

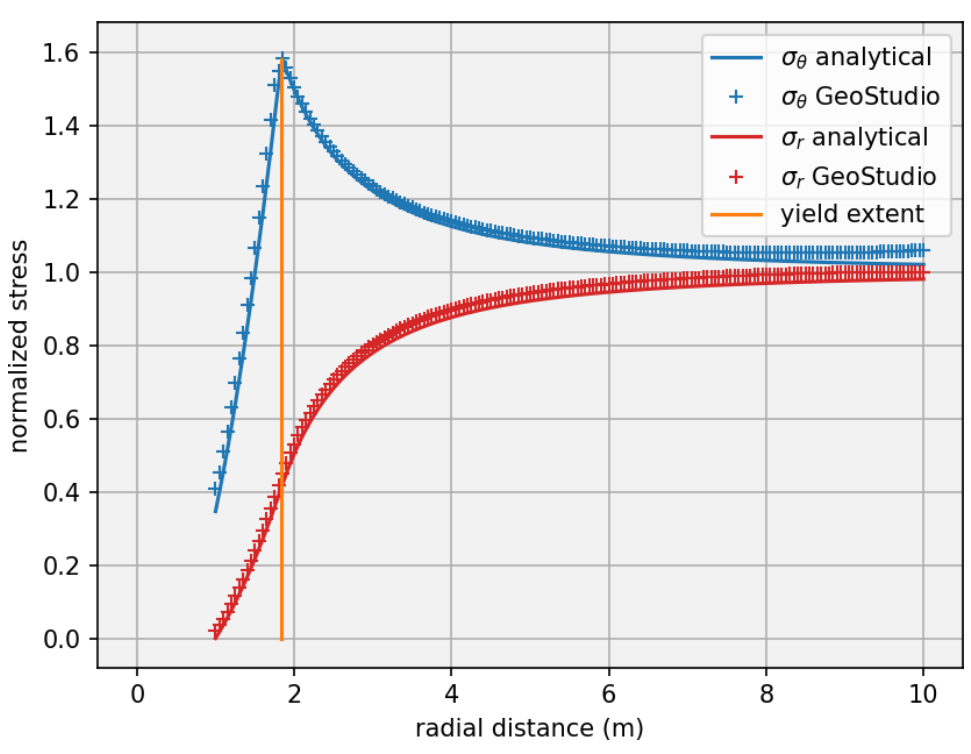


Figure 10. Normalized radial and tangential stress versus radial distance. Associated flow, dilation = 30°.



References

Salençon, J. "Contraction Quasi-Statique D'une Cavite a Symetrie Spherique Ou Cylindrique Dans Un Milieu Elastoplastique," Annales Des Ponts Et Chaussees, 4, 231-236 (1969).

